

COLLECTIVE PHENOMENA WITH ENERGETIC PARTICLES IN FUSION PLASMAS *

B.N. BREIZMAN, H.L. BERK, J. CANDY, M.S. PEKKER, N.V. PETVIASHVILI, J.W. VAN DAM, H.V. WONG

Institute for Fusion Studies, The University of Texas at Austin, Austin, TX 78712, USA

Z.Y. CHANG, E. FREDRICKSON, G.Y. FU, K.L. WONG

Plasma Physics Laboratory, Princeton University, Princeton, NJ 08543, USA

A. FASOLI

Plasma Science and Fusion Center, Massachusetts Institute of Technology, Cambridge, MA 02139, USA

D. BORBA, R.F. HEETER, S.E. SHARAPOV

JET Joint Undertaking, Abingdon OX14 3EA, United Kingdom

F. PORCELLI

Departamento di Energetica, Politecnico di Torino, Torino 10129, Italy

V.P. PASTUKHOV

Russian Research Center "Kurchatov Institute," Moscow 123182, Russia

Abstract

Recent progress in the theory of collective modes driven by energetic particles, as well as interpretations of fast particle effects observed in fusion-related experiments, are described. New developments in linear theory include: (a) Alfvén-mode frequency gap widening due to energetic trapped ions, (b) interpretation of JET results for plasma pressure effect on TAE modes, and (c) "counter" propagation of TAE modes due to trapped fast ion anisotropy. The new nonlinear results are: (a) theoretical explanation for the pitchfork splitting effect observed in TAE experiments on JET, (b) existence of coherent structures with strong frequency chirping due to kinetic instability, (c) self-consistent nonlinear theory for fishbone instabilities, and (d) intermittent quasilinear diffusion model for anomalous fast particle losses.

1. ALFVÉN FREQUENCY GAP WIDENING

High-frequency Alfvén modes, apparently excited by fast ions, were observed during H-minority ion cyclotron heating experiments on TFTR [1]. The mode frequency, which scales as $n_e(0)^{-1/2}$, consistent with Alfvénic fluctuations, is approximately twice the TAE frequency, as shown in Fig. 1. The high-frequency modes, seen with and also without accompanying TAE activity, were observed when the H-minority ICRF resonance was slightly off axis on the high field side ($R_{\text{res}}^{\text{RF}}=2.35$ m, whereas $R_0=2.62$ m). The experimental parameters were $I_p=1.3$ MA, $B_{\text{tor}}=2.5$ T, and $a_p=0.97$ m. With 4 MW of RF power at $f_{ci}^{\text{RF}}=43$ MHz, 90% of the plasmas exhibited these modes.

The high-frequency modes are in good agreement with the predicted frequency and radial location for an Alfvén eigenmode in the "second" spectral gap, which is opened by ellipticity. However, this result is surprising, since the TFTR cross section is circular, so that the second spectral gap is very narrow, with width of order $(r/R_0)^2$. These high-frequency modes had not been observed previously in hundreds of on-axis H-minority ICRH experiments. A proposed explanation is based on a theory showing that the presence of an energetic trapped-ion population in a tokamak plasma can broaden the width of the frequency gaps in the shear Alfvén spectrum [2]. This new effect is in addition to the usual geometrical effects such as toroidicity or noncircularity and sometimes exceeds them in magnitude.

* Work at IFS performed under U.S. DOE Contract No. DE-FG03-96ER54346 and at PPPL under U.S. DOE Contract No. DE-AC02-76-CHO-3073.

The best experimental fits to the 7-coil toroidal array of Mirnov coils give the mode number $n=4$ and also indicate that these modes propagate opposite to the plasma ion diamagnetic frequency, contrary to usual TAE modes and the related Fast Ion Modes. Initial calculations of the fast ion pressure profile show that it is hollow at the mode location ($r/a \approx 0.3$), hence consistent with “backwards” mode propagation. Instability requires that the magnetic precessional drift frequency also be reversed in direction, which is predicted to occur for barely-trapped fast ions, with poloidal turning points $|\theta_t| \geq 3\pi/4$, consistent with the off-axis heating on the high-field side in the experiments. Detailed calculations of the damping and driving terms remain to be done.

2. FINITE-BETA SUPPRESSION OF TAE MODES

In high-performance JET hot-ion H-mode deuterium discharges, the measured amplitudes of TAEs excited by ICRF-heated fast ions gradually decrease in time and disappear completely at the peak fusion performance [3]. Both ICRH and NBI heating powers remain constant during the observation period. Analysis with the PION code indicates that the total energy content of ICRF-heated protons does not decrease, nor does the energy content of the part necessary for TAE excitation (i.e., the proton tail with $E > 500$ keV).

In order to understand the evolution of the ICRH-driven TAEs, the JET plasma equilibria were reconstructed with the EFIT and HELENA codes at different time slices. Accuracy of the reconstructed safety factor profile $q(r)$ was checked at the TAE values $q = (m + \frac{1}{2})/n$ through a comparison of the TAE Doppler shift measurements with the profile of the differential toroidal plasma rotation measured by charge-exchange diagnostic. Subsequently, the MISHKA code was used for normal-mode analysis of the reconstructed equilibria.

Core-localized TAE modes computed by the ideal-MHD version of MISHKA agree well, to within 10–17% accuracy, with the measured TAE frequencies. The computed radial width of the TAE modes shrinks in time with increasing plasma pressure gradient, and no core-localized TAEs are found when the normalized plasma pressure gradient $\alpha = -R_0 q^2 (d\beta/dr)$ exceeds the critical value [4, 5] $\alpha_{crit} = \varepsilon + 2\Delta' \pm S^2 \approx 3\varepsilon \pm 2S^2$. Here, $S = (r/q)(dq/dr)$ is the magnetic shear, β the toroidal plasma beta, Δ' the Shafranov shift, and $\varepsilon = r/R_0$.

The finite-beta suppression of TAE modes was also analyzed from the perspective of non-ideal MHD by use of the MISHKA code that includes complex resistivity, which can model first-order ion finite Larmor radius effects at the TAE gap location. The computed time evolution of the TAE modes exhibits increasing radiative damping, from $(\gamma/\omega)_{rad} = 0.72\%$ at the beginning of TAE observation to $(\gamma/\omega)_{rad} = 2.6\%$ at the end. Hence the explicit reason why core-localized TAE modes cannot exist is their large radiative damping. The MISHKA modeling shows that nonideal kinetic-TAEs are the only Alfvén eigenmodes that persist at the time of highest plasma performance; however, kinetic-TAEs have anti-ballooning mode structure and hence do not interact with ICRH-generated trapped ions.

3. TAE “COUNTER” PROPAGATION DUE TO FAST-ION ANISOTROPY

Occasionally, TAE modes excited by ICRF-heated tail ions are observed to “counter” propagate, i.e., with phase velocity opposite to the direction of the thermal ion diamagnetic velocity. A natural explanation—if instability arises primarily from the universal drive (spatial gradient of the fast particle distribution)—would be that the resonant particles have a hollow radial profile. However, here we offer another possible explanation, associated with the strong anisotropy produced in ICRH plasmas.

With ICRH, particles whose turning points are in the neighborhood of the cyclotron resonance surface are preferentially heated. Hence the distribution function is sharply peaked in pitch angle, resulting in an inverted energy population (at constant magnetic moment) for many of the heated particles. Particle anisotropy thus provides another source of free energy in addition to the universal instability drive, and under certain conditions, it is more effective in destabilizing counter-propagating TAE modes than co-propagating TAE modes.

Wave-particle resonance requires that the mode frequency be equal to the sum of an integer multiple of the toroidal drift frequency (proportional to the square of the particle velocity) and an integer multiple of the trapped particle bounce frequency (proportional to the particle velocity). Thus, for a given bounce harmonic number, there can be up to two physical solutions for the resonant particle velocity. However, in the case of co-propagation, there is only one relevant

solution at each bounce harmonic resonance, and the effect of particle anisotropy is to enhance, in an expected way, the usual universal instability drive and significantly reduce the threshold for the onset of instability. On the other hand, in the case of counter-propagation, for a given bounce harmonic there are either two or zero physical solutions possible for the resonant velocity, depending on the frequency of the wave. At a critical frequency, the two roots coalesce, and one finds that if Alfvén waves can be excited near this frequency, then, surprisingly, the growth rates for counter-propagation are considerably larger than those found for co-propagation (Fig. 2).

4. PITCHFORK SPLITTING

In a number of JET discharges, Alfvén eigenmodes are excited by a small population of ICRF-heated fast hydrogen ions. These experiments have revealed an intricate nonlinear phenomenon: the excited mode exhibits a sequence of bifurcations, the first being a transition from a single spectral line to several closely spaced spectral components, as shown in Fig. 3 (“pitchfork” splitting effect) [6].

Our interpretation of this phenomenon is based on a first-principles theoretical model for near-threshold kinetic instabilities [7]. The key idea of the model is that the system cannot go far beyond the instability threshold because the source of energetic particles is relatively weak, so that the population of fast ions builds up on a much longer time scale than the characteristic growth time of the instability. The evolution of the unstable mode in this regime is governed by the resonant wave-particle interaction and the collision-like relaxation process for resonant particles that can be characterized by an effective collision frequency v_{eff} . Near the instability threshold, the mode linear growth rate γ (the difference between the energetic particle drive γ_L and the background damping rate γ_d) is small compared with both γ_L and γ_d . Even a relatively small nonlinear correction to γ_L can then compete with this small difference. This feature allows us to treat the nonlinearity perturbatively by expanding the energetic particle response in powers of the mode amplitude A and retaining only the lowest order nonlinear contribution. The resulting nonlinear equation for the mode amplitude A has the form [7]:

$$\exp(-i\phi) \frac{dA}{dt} = \frac{\gamma}{\cos\phi} A - \frac{\gamma_L}{2} \int_0^{t/2} \tau^2 d\tau \int_0^{t-2\tau} d\tau_1 \exp[-v_{eff}^3 \tau^2 (2\tau/3 + \tau_1)] \times A(t-\tau)A(t-\tau-\tau_1)A^*(t-2\tau-\tau_1), \quad (1)$$

where the parameter ϕ , whose value is on the order of γ_L/ω , characterizes the fast particle contribution to the real part of the mode frequency ω . Apart from a numerical factor, $|A|$ is equal to the square of the nonlinear bounce frequency, ω_b^2 , for a typical resonant particle trapped in the wave. The neglect of higher order terms in Eq. (1) is valid since the mode saturates before the resonant particles complete a bounce period in the perturbed field. The structure of Eq. (1) indicates that the saturated amplitude must scale as $\gamma^{1/2}$. The corresponding value of ω_b in the saturated state turns out to be smaller than v_{eff} , i. e., particles decorrelate from the resonance before their motion becomes strongly nonlinear. It follows from the solution of Eq. (1) that the mode converges dynamically to a steady saturated state when γ is sufficiently small. However, this saturated state becomes unstable and bifurcates when γ exceeds a critical value γ_{cr} , equal to $0.486v_{eff}$ for $\phi \ll 1$. Above this threshold, the solution is a periodic limit-cycle: $A = A_0 \exp(i\delta\omega t)[1 + \alpha_1 \exp(i\Delta\omega t) + \beta_1^* \exp(-i\Delta\omega t) + \alpha_2 \exp(i2\Delta\omega t) + \beta_2^* \exp(-2i\Delta\omega t) + \dots]$, where A_0 and $\delta\omega$ are the amplitude and nonlinear frequency shift of the main spectral component, $\Delta\omega$ is the sideband frequency, and α_i and β_i are the relative amplitudes of the sidebands. Equation (1) leads to the following relationship between γ_{cr} , v_{eff} , and $\Delta\omega$ at the bifurcation point: $\Delta\omega = 1.18\gamma_{cr} = 0.575v_{eff}$. As γ/v_{eff} increases past the first bifurcation, the limit cycle solution exhibits further bifurcations leading to period doublings. This is illustrated by Fig. 4, which shows the power spectra of the function $A(t)$ for three values of γ/v_{eff} .

The nonlinear saturated states described by Eq. (1) match the experimental spectra shown in Fig. 5, in which the splitting of the initial spectral line and the subsequent period-doubling bifurcation are both clearly seen. In the experiment, the time between the beginning of the TAE signal and the first bifurcation is short compared to the total duration of the instability and the fast particle slowing-down time. Hence, in this initial interval, the evolution of the growth rate γ can be approximated as a linear function of time and v_{eff} treated as a constant. With this assumption, the evolution of the mode amplitude was computed from Eq. (1) over a time interval including the

first bifurcation. To provide a seed for instability and to simulate the observed noise level, a small random source term was added to the right-hand side of Eq. (1). Figure 6 shows that the experimental data (JET discharge #40328) for the time evolution of the central line and the up- and down-shifted sidebands for the $n=7$ TAE mode is well reproduced by the simulation results with $\phi = 3\pi/64$ over this time interval.

In our theory, the frequencies and amplitudes of the nonlinear sidebands are determined by the values of the growth rate γ_{cr} and the effective collision frequency ν_{eff} —which relationship may provide a very accurate way to obtain these values. Indeed, the inferred value of the growth rate is consistent with previous measurements of the ICRH drive for low- n TAE modes [8]. The inferred value of ν_{eff} is several times larger than the effective collision frequency as calculated from pitch angle scattering due to Coulomb interactions. However, the enhanced collisionality can be attributed to velocity space diffusion induced by the ICRH wave fields, which dominates over that due to Coulomb collisions in high-temperature plasmas. Thus, in principle, from the value of ν_{eff} one could then infer the fast particle diffusion coefficient due to ICRH and obtain information about the intensity of the ICRH wave field.

5. COHERENT STRUCTURES WITH STRONG FREQUENCY CHIRPING

The steady state and limit cycle regimes of mode saturation described in Sec. 4 require the growth rate γ to be smaller than or comparable to the relaxation rate ν_{eff} . When γ is larger than ν_{eff} , the solution of the truncated cubic nonlinear equation, Eq. (1), does not saturate. Instead, the amplitude A grows to infinity in a finite time, with simultaneous oscillations at increasing frequency. Equation (1) fails when A approaches γ_L^2 . Hence, to determine how the solution evolves beyond the explosive phase, the Vlasov equation with a Fokker-Planck diffusion term was solved simultaneously with the wave evolution equation [9]. The specific example discussed in Ref. [9] is for the simplified case of the bump-on-tail instability, but similar results arise when the TAE mode is simulated with a particle code [10].

We find that the mode saturation level is determined by the condition that the trapping frequency of particles in the wave is comparable to γ_L . We also discover the surprising result that the explosive phase is followed by an adiabatic phase in which the saturated state persists for times long compared to the inverse linear damping rate, and that the sideband frequencies continue to shift upward and downward by an amount substantially larger than γ_L after saturation is reached. The numerical simulation shows that a hole and a clump are formed in the particle distribution function [9]. The hole and clump support a pair of BGK nonlinear waves, which persist for a long time because the background dissipation is balanced by the frequency sweeping process that extracts energy from the fast particles skimming past the moving phase space structures. The self-consistent BGK solution [9] has ω_b comparable to γ_L and an arbitrary time-dependent frequency shift. As the frequency shift $\delta\omega$ changes in time, the phase space hole moves upward in energy and the clump moves downward. The motion of the phase space structures releases power, proportional to $\gamma_L \omega_b \delta\omega d(\delta\omega)/dt$, which should be set equal to the dissipated power $\gamma_d \omega_b^4$. This power balance, together with the condition $\omega_b \approx \gamma_L$, determines the time dependence of the frequency shift as $\delta\omega \approx \gamma_L (\gamma_d t)^{1/2}$. Figure 7 shows the spatially averaged distribution function as a function of velocity and time and the power spectrum as a function of frequency and time. Note that the peaks of the spectral power coincide with the depression (phase space hole) and the hill (phase space clump) on the averaged distribution function. The mode persists until diffusion destroys the phase space structures on a time scale γ_L^2 / ν_{eff}^3 . Interestingly, the hole-clump pair does not spontaneously arise when the system is far above the instability threshold. In this case there is no explosive phase to initiate chirping and separate the hole and clump; instead, the distribution function merely flattens in the resonance region, after which the wave damps away at the background damping rate.

Hole-clump pairs were also observed in particle simulations of TAE modes destabilized by toroidally trapped fast ions. This instability involves many simultaneous wave-particle resonances at different energies. Figure 8, which is a contour plot of the power spectrum of the perturbations after saturation of linear growth, displays the time variation of the hole and clump frequency shifts of the dominant modes. These frequency shifts agree with the theoretical prediction $\Delta\omega / \gamma_L = \pm 0.43(\gamma_L t)^{1/2}$ (dotted curves in Fig. 8).

6. NONLINEAR FISHBONE DYNAMICS

The fishbone instability has long been recognized to result from fast particle interaction with the $m=n=1$ internal kink perturbation. Characteristic features of this instability are its explosive growth and the frequency sweeping effect, both of which are clearly nonlinear phenomena. Motivated to simulate this behavior, we have developed a physical model of the fishbone instability that self-consistently treats the wave-particle nonlinearity together with the linear $q=1$ layer response [11]. This model has been coupled to a δf particle code to allow a precise calculation of the nonlinear energetic particle current in general geometry. The resulting code has been applied to the simulation of fishbone oscillations in a JET-like plasma, as well as in larger reactor-grade plasmas.

Since the kink displacement is rigid away from the $q=1$ surface, a reduced dynamical equation for the on-axis radial displacement $\xi_0(t)$ can be constructed [11]. The result takes the symbolic form $F_{\text{bulk}}[\xi_0(t)] = \Lambda_K[\xi_0(t)]$. The temporally nonlocal operator F_{bulk} , computed analytically, describes all the linear physics of the bulk plasma. The term Λ_K which represents the response of the fast particles, is a functional of their perturbed distribution function f_{fast} , which in turn is a nonlinear functional of $\xi_0(t)$. To compute f_{fast} , the exact nonlinear guiding-center trajectories are followed in the presence of a fixed-shape (top-hat-like) perturbation with self-consistently evolving amplitude $\xi_0(t)$. Our simulation results reproduce the explosive (i.e., faster than exponential) scaling $\xi_0(t) \propto (t_0 - t)^{-5/2}$ during the onset of the instability in a reactor-size plasma [12]. The explosive behavior was verified near marginal stability in both the lower-frequency ($\omega < \omega_{*i}$) regime of diamagnetic fishbone modes and the higher-frequency ($\omega > \omega_{*i}$) regime of precessional fishbone modes.

The code was also applied to a JET-like plasma with parameters characteristic to auxiliary-heated discharges: $\omega_{*i} = 10^4$ rad/s, $T_{\text{fast}} = 80$ keV (with fast ions assumed to be fully isotropic), and $\beta_{\text{fast}} = 0.5\%$. The result, shown in Fig. 9, was a burst about 10 ms in duration, with significant frequency chirping, both features being typical of JET discharges [13].

In order to bring the fishbone simulations closer to reality, our model needs to be generalized to incorporate fluid nonlinearities of the resonant layer near the $q=1$ surface. This work is now in progress. As a first step in this direction we have evaluated the role of fluid nonlinearities analytically in the near-threshold limit where they can be treated perturbatively. These calculations lead to an equation similar to Eq. (1) but now with two cubic nonlinear terms, one of which describes the kinetic nonlinearity and the other the ideal-MHD nonlinearity. The ratio of the ideal-MHD contribution to the kinetic contribution is roughly on the order of $(sV_A / \omega R)^2 (r_{\text{fast}} / r_1)^2$, where s is the magnetic shear at the $q=1$ surface, V_A is the Alfvén velocity, R is the major radius, ω is the mode frequency, r_{fast} is the radial scale length of the hot particle distribution and r_1 is the radius of the $q=1$ surface. It follows from the weakly nonlinear analysis that the ideal-MHD nonlinearity rather than the energetic particle nonlinearity controls the explosive growth of the mode at the onset of the fishbone pulse. The relative role of the two nonlinearities during the saturation and during the decay of the pulse still must be assessed. However, it is conceivable that, with sufficient viscosity, the ideal-MHD nonlinearity becomes less significant or even negligible because of resonance layer broadening. The value of viscosity that is required to suppress the ideal-MHD nonlinearity appears to be moderate if one takes into account that the kinetic effects alone, as described by the code, eventually lead to mode saturation at a level as surprisingly low as that indicated in Fig. 9.

7. INTERMITTENT MODEL FOR ANOMALOUS FAST PARTICLE LOSSES

A single weakly unstable mode rarely causes strong losses of fast particles since it only affects a relatively small near-resonant area of phase space. Anomalous losses are usually associated with multiple modes that lead to global quasilinear diffusion. However, quasilinear diffusion requires the mode amplitudes to be sufficiently large to satisfy the resonance overlap condition. In the presence of background damping, a weak source of energetic particles may not be able to continuously maintain this critical level of turbulence. On the other hand, given enough time without anomalous transport, the same weak source may create an inverted population of particles with sufficient free energy to trigger the overlap. This situation leads to an interesting regime of intermittent quasilinear diffusion when turbulent bursts and losses are followed by quiescent periods during which the system accumulates free energy needed for the next burst. It is essential that each burst releases much more energy than what would be released by a set of

isolated resonances. Once triggered, the burst forces the mean gradient of the particle distribution to fall somewhat below the threshold of linear instability, which explains the decay of turbulence at the end of the burst.

In this vein we consider a simple model with the following set of quasilinear equations,

$$\frac{\partial f}{\partial t} - \frac{\partial}{\partial \Omega} D \frac{\partial f}{\partial \Omega} = -\nu(f - f_0), \quad \frac{\partial D}{\partial t} = \left(\frac{\partial f}{\partial \Omega} - \gamma_d \right) D, \quad (2)$$

in the domain $0 < \Omega < \Omega_{\max}$, with boundary conditions $f|_{\Omega=0} = 0$ and $D \partial f / \partial \Omega|_{\Omega=\Omega_{\max}} = 0$. If we take $f_0 = \Omega \gamma_L$, then in the absence of waves, a distribution function will build up to $f = f_0$. However, if $\gamma_L > \gamma_d$ and waves are present, a steady solution is found where $f = \Omega \gamma_d$, and D is given by $D \equiv \nu \gamma_L \Omega^2 / \gamma_d$. This solution indicates that diffusion in the unstable spectrum limits the build-up of the energetic population, but it does not explain pulsations that generally accompany experiments. Pulsations arise in the theory if we assume that there are a discrete number, N , of active modes, and that these modes are roughly evenly spaced in Ω . Then it is readily shown that mode overlap requires $D > (\Omega/N)^3$. Hence if $\nu \gamma_L / (\Omega \gamma_d) < 1/N^3$ the steady state quasilinear equation cannot be satisfied. Then the weak source, νf_0 , can drive the distribution function above the marginal stability level, because only benign single mode excitations arise, which do not limit the further build-up of the distribution. If $\gamma_L < \Omega/N^3$, the distribution f can approach its maximum value f_0 . If $\gamma_L > \Omega/N^3 > \gamma_d$, the distribution will build up well above marginal stability, but it is subject to a catastrophic collapse, with loss of nearly all particles since the quasilinear equations now allow a solution with $D \geq (\Omega/N)^3$, where total particle loss occurs in a time less than γ_d^{-1} . It will take a relatively long time, $T_{\text{recovery}} \cong \Omega / (\gamma_L N^3 \nu)$, for the distribution to build up until the next pulse takes place. However, if $\nu \gamma_L / \gamma_d^2 < \Omega / (\gamma_d N^3) < 1$, the quasilinear equation with the constraint $D \geq (\Omega/N)^3$ predicts wave evolution with short pulses and small loss fractions for each pulse. In this case, the energetic particles build up to slightly above the marginal stability level and fall somewhat below this level with each pulsation. A fraction $\varepsilon \cong [\Omega / (\gamma_d N^3)]^{1/2}$ of particles are lost during a short turbulent pulse interval, $T_{\text{pulse}} \sim N^{3/2} / (\Omega \gamma_d)^{1/2}$, and a longer recovery time, $T_{\text{recovery}} \sim (\Omega \gamma_d / N^3)^{1/2} / \nu \gamma_L \propto D^{1/2}$, is needed before the instability is re-triggered.

This discrete mode modification of the solution of the quasilinear equations has pulsation characteristics similar to those of the heuristic predator-prey model [15]. However, in the quasilinear model with discrete modes, basic physics principles govern the dynamics.

Our picture of intermittent global diffusion has features that are characteristic of beam losses produced by toroidal Alfvén eigenmodes in TFTR [16] and DIII-D [17]. This avalanche-type scenario is not limited to the problem of fast particle transport, but should be applicable as well to the more general problem of turbulent transport.

REFERENCES

- [1] FREDRICKSON, E., CHANG, Z., FU, G.Y., "Observation of Modes at Frequencies Near the 2nd Alfvén Gap in TFTR," Proc. IEA Tripartite Workshop on TAE Modes and Energetic Particle Physics: W36, Naka, 25-27 February 1997 (Japan Atomic Energy Research Institute, Naka, Japan, May 1997), p. 327.
- [2] ROSENBLUTH, M.N., VAN DAM, J.W., unpublished notes.
- [3] SHARAPOV, S.E., BORBA, D., FASOLI, A., KERNER, W., ERIKSSON, L.-G., HEETER, R.F., HUYSMANS, G.T.A., MANTSINEN, M.J., "Stability of Alpha Particle Driven Alfvén Eigenmodes in High Performance JET DT Plasmas," submitted to Nucl. Fusion.
- [4] FU, G.Y., Phys. Plasmas **2** (1995) 1029.
- [5] BERK, H.L., VAN DAM, J.W., BORBA, D., CANDY, J., HUYSMANS, G.T.A., SHARAPOV, S.E., Phys. Plasmas **2** (1995) 3401.
- [6] FASOLI, A., BREIZMAN, B.N., BORBA, D., HEETER, R.F., PEKKER, M.S., SHARAPOV, S.E., "Nonlinear Splitting of Fast Particle Driven Alfvén Eigenmodes: Observation and Theory," submitted to Phys. Rev. Lett. (1998).
- [7] BERK, H L, BREIZMAN, B N., PEKKER, M.S., Plasma Phys. Reports **23** (1997) 778.
- [8] FASOLI, A., BORBA, D., GORMEZANO, C., et al., Plasma Phys. Contr. Fusion **39** (1997) B287.
- [9] BERK, H.L., BREIZMAN, B.N., PETVIASHVILI, N.V., Phys. Lett. A **234** (1997) 213 (1997); *ibid.* **238** (1998) 408.
- [10] WONG, H.V., BERK, H.L., Phys. Plasmas **5** (1998) 2781.
- [11] BREIZMAN, B.N., CANDY, J., PORCELLI, F., BERK, H.L., Phys. Plasmas **5** (1998) 2326.

- [12] CANDY, J., PORCELLI, F., BERK, H.L., BREIZMAN, B.N., “Nonlinear Theory of Internal Kink Modes Destabilized by Fast Ions in Tokamak Plasmas,” Proc. 25th European Physical Society Conference, Prague, 1998.
- [13] NAVE, M.F.F., et al., Nucl. Fusion **31** (1991) 697.
- [14] PASTUKHOV, V.P., BREIZMAN, B.N., PEKKER, M., “Weakly Nonlinear Regime of Fishbone Instability,” Bull. Am. Phys. Soc. (1998).
- [15] HEIDBRINK, W.W., et al., Phys. Fluids B **5** (1993) 2176.
- [16] WONG, K.L., et al., Phys. Rev. Letters **66** (1991) 1874.
- [17] HEIDBRINK, W.W., et al., Nucl. Fusion **31** (1991) 1635.

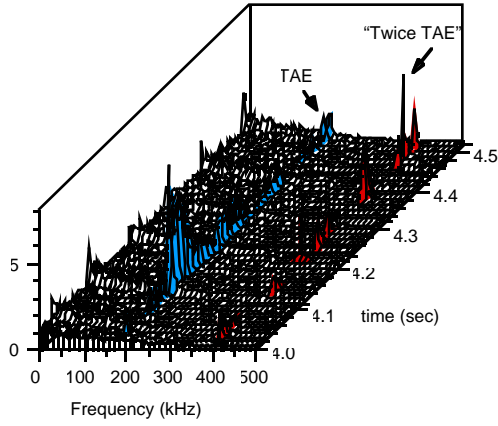


FIG. 1. TAE and “second gap” Alfvén modes seen in TFTR H-minority ICRH experiments.

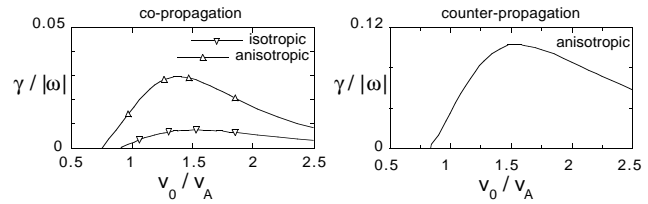


FIG. 2. TAE growth rate due to anisotropy drive, for co- and counter-propagating modes (note the different scales).

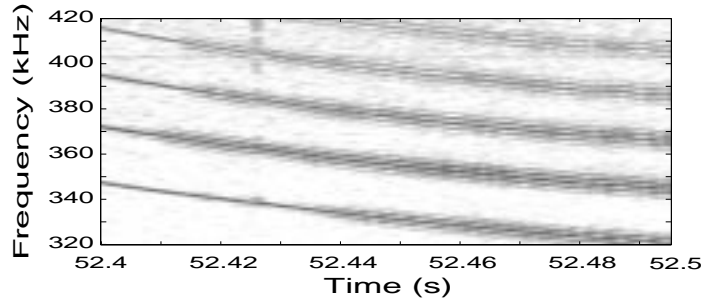


FIG. 3. Pitchfork splitting of TAE modes in JET (experimental results from Mirnov coils).

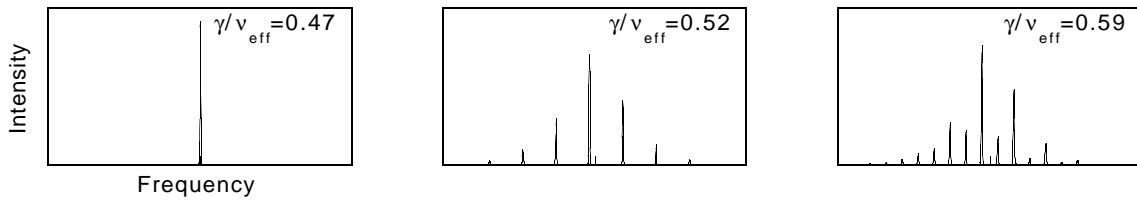


FIG. 4. Snapshots of the power spectrum of the saturated solution of Eq. (1), with $\phi=3\pi/64$, showing nonlinear spectral line splitting and the period-doubling bifurcation.

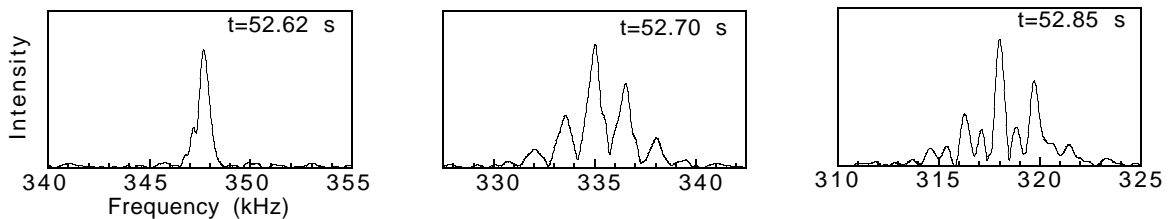


FIG. 5. Snapshots of the $n=7$ toroidal Alfvén eigenmode magnetic activity in JET discharge #40238.

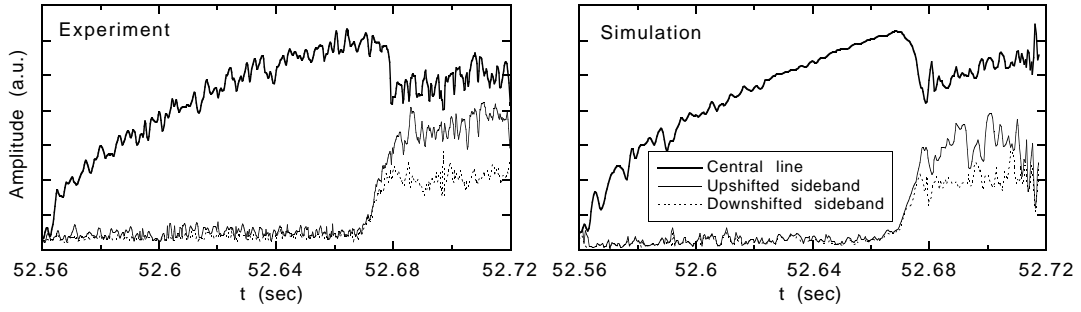


FIG. 6. Time evolution of the $n=8$ mode spectral components (JET shot # 40328) showing bifurcation and nonlinear splitting at $t=52.67$ sec. Left plot: experimental data. Right plot: simulation results with $\gamma=7.85 \cdot 10^4 (t-52.56) \text{ s}^{-1}$, $v_{\text{eff}}=1.78 \cdot 10^4 \text{ s}^{-1}$, and $\phi=3\pi/64$.

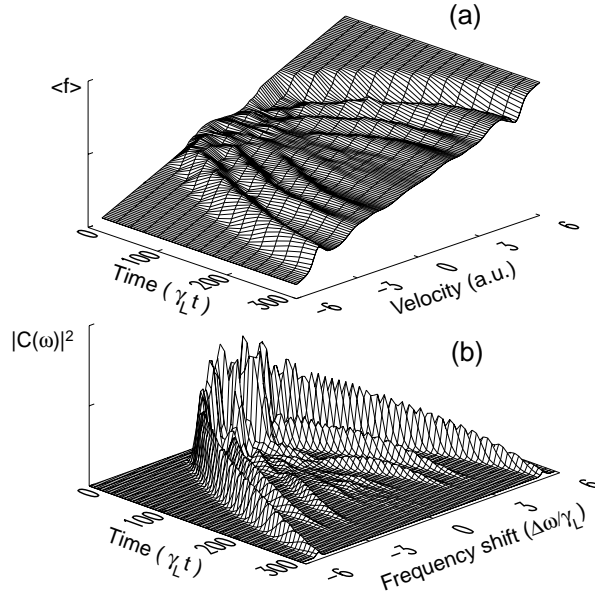


FIG. 7. Formation of hole-clump structures with time-dependent frequencies in the near-threshold regime for the bump-on-tail instability: (a) spatially-averaged particle distribution function, (b) wave power spectrum.

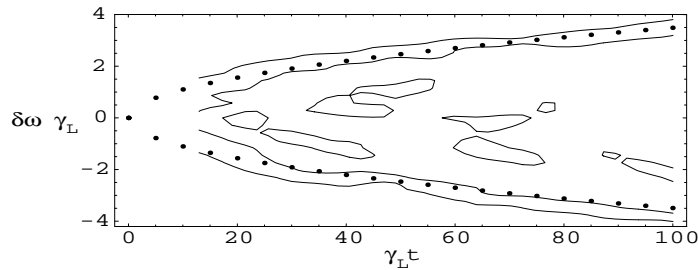


FIG. 8. Hole-clump frequency chirping in time for TAE modes, compared with theory (dotted curves).

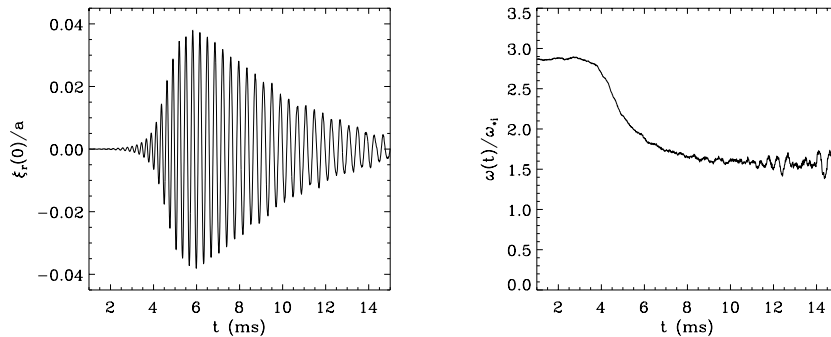


FIG. 9. On-axis displacement (left) and frequency (right) of a simulated fishbone burst in a JET-like plasma.